1-1-2022

Uveitis-mediated immune cell invasion through the extracellular matrix of the lens capsule

JodiRae DeDreu
Thomas Jefferson University

Sonali Pal-Ghosh
George Washington University School of Medicine and Health Sciences

Mary J Mattapallil
National Institutes of Health

Rachel R Caspi
National Institutes of Health

Mary Ann Stepp
George Washington University School of Medicine and Health Sciences

See next page for additional authors

Authors
JodiRae DeDreu, Sonali Pal-Ghosh, Mary J Mattapallil, Rachel R Caspi, Mary Ann Stepp, and A Sue Menko

Received: 2 July 2021 | Revised: 20 September 2021 | Accepted: 4 October 2021

DOI: 10.1096/fj.202101098R

THE FASEB JOURNAL

RESEARCH ARTICLE

Uveitis-mediated immune cell invasion through the extracellular matrix of the lens capsule

JodiRae DeDreu[1] | **Sonali Pal-Ghosh**[2] | **Mary J. Mattapallil**[3] | **Rachel R. Caspi**[3] | **Mary Ann Stepp**[2,4] | **A. Sue Menko**[1,5]

[1]Department of Pathology, Anatomy and Cell Biology, Sidney Kimmel Medical College, Thomas Jefferson University, Philadelphia, Pennsylvania, USA

[2]Department of Anatomy and Cell Biology, George Washington University School of Medicine and Health Sciences, Washington, District of Columbia, USA

[3]Laboratory of Immunology, National Eye Institute, National Institutes of Health, Bethesda, Maryland, USA

[4]Department of Ophthalmology, George Washington University School of Medicine and Health Sciences, Washington, District of Columbia, USA

[5]Department of Ophthalmology, Sidney Kimmel Medical College, Thomas Jefferson University, Philadelphia, Pennsylvania, USA

Correspondence
A. Sue Menko, Department of Pathology, Anatomy and Cell Biology, Co-Director, Wills Vision Research Center at Jefferson, Thomas Jefferson University, 564 Jefferson Alumni Hall, 1020 Locust Street, Philadelphia, PA 19107, USA.
Email: sue.menko@jefferson.edu

Funding information
HHS | NIH | National Eye Institute (NEI), Grant/Award Number: EY021784

Abstract

While the eye is considered an immune privileged site, its privilege is abrogated when immune cells are recruited from the surrounding vasculature in response to trauma, infection, aging, and autoimmune diseases like uveitis. Here, we investigate whether in uveitis immune cells become associated with the lens capsule and compromise its privilege in studies of C57BL/6J mice with experimental autoimmune uveitis. These studies show that at D14, the peak of uveitis in these mice, T cells, macrophages, and Ly6G/Ly6C+ immune cells associate with the lens basement membrane capsule, burrow into the capsule matrix, and remain integrated with the capsule as immune resolution is occurring at D26. 3D surface rendering image analytics of confocal *z*-stacks and scanning electron microscopy imaging of the lens surface show the degradation of the lens capsule as these lens-associated immune cells integrate with and invade the lens capsule, with a subset infiltrating both epithelial and fiber cell regions of lens tissue, abrogating its immune privilege. Those immune cells that remain on the surface often become entwined with a fibrillar net-like structure. Immune cell invasion of the lens capsule in uveitis has not been described previously and may play a role in induction of lens and other eye pathologies associated with autoimmunity.

KEYWORDS

basement membrane, immune cell attachment, immune cell infiltration, immune cell migration, immune privilege, inflammation, lens, matrix, uveitic

Abbreviations: EAU, experimental autoimmune uveitis; MAGP1, microfibril associated protein-1; MDSC, myeloid-derived suppressor cells; MMP, matrix metalloproteinase; PCO, posterior capsule opacification; SEM, scanning electron microscopy; αSMA, alpha smooth muscle actin.

Mary Ann Stepp and A. Sue Menko are Co-Senior Authors.

1 | INTRODUCTION

The avascular properties of tissues in the central light path of the eye, like the lens, create an ocular environment long classified as immune privileged.[1] This privilege is abrogated in autoimmune diseases such as uveitis and diabetes, and can lead to blindness.[2] Uveitis often occurs following injuries to or infections of the eye[3] and is also a consequence of autoimmune or other inflammatory disorders that occur outside of the eye, such as spondyloarthropathies.[4–6] In uveitis, an inflammatory intraocular disease with an adaptive immune component,[2] immune cells populate many different regions of the eye where inflammation results in destructive effects.[2,7–9] The most common type is anterior uveitis, with other forms classified as intermediate (primarily vitreous), posterior (retina and choroid), and panuveitis (across many regions of the eye).[10–12] When untreated, uveitis can result in the scarring, swelling or detachment of the retina, damage to the optic nerve, and glaucoma, as well as lens cataract.[2,12,13] Uveitis is also clinically linked to many post-cataract surgery complications, including the lens fibrotic disease Posterior Capsule Opacification (PCO), glaucoma, macular edema, and retinal detachments.[14–18]

The aqueous and vitreous humors, both compartments in which inflammatory cells are prominent in uveitis, are in direct contact with the lens. The aqueous humor, a proteinaceous fluid whose composition is similar to that of arterial plasma, occupies the anterior chamber of the eye.[19–21] The vitreous humor is a gel-like, extracellular matrix-rich substance that occupies the posterior chamber in the space between the lens and the retina.[22,23] Autoimmune diseases like uveitis and diabetes have long been associated with the development of eye pathologies that include lens cataracts.[13] However, the possibility that the immune cells present in the environment of the lens could invade the lens capsule in these and other inflammatory conditions had not been previously considered. The lack of previous studies has stemmed from the fact that the lens is an avascular tissue and the belief that its basement membrane capsule provides a barrier to immune cells that confers the lens with immune privilege.

The finding that immune cells become associated with and then invade the superficial surface of the lens basement membrane capsule within one day post-cornea wounding injury[24] raised the possibility that inflammatory cells in the environment of the lens in autoimmune diseases like uveitis can also associate with this tissue. In the corneal wounding scenario, the lens-associated immune cells travel from the vascular-rich ciliary body along the avascular zonule fibrils that anatomically link these two tissues, from where they then associate with the equatorial and anterior surfaces of the lens.[24] The subset of immune cells that migrate along the lens capsule surface in response to corneal injury include macrophages/monocytes and neutrophils. In a longer-term study with a lens conditional N-cadherin knockout mouse (N-cad$^{\Delta lens}$), in which the absence of N-cadherin results in fiber cell degeneration and cataract-like opacities, it was discovered that an adaptive immune response is induced in which macrophages, B cells and T cells populate the lens.[25] These immune cells, which access the lens across an intact lens capsule, were found to be highly susceptible to acquiring a myofibroblast phenotype and were linked to the accumulation of collagen I in the region of lens fiber cell degradation that they populate.[25] The development of this immune cell-linked fibrosis is likely responsible for the observed lens opacities in this knockout mouse.

There is a high incidence of lens opacities in patients with uveitis, including cortical, nuclear and posterior subcapsular cataracts.[13,26–28] While the mechanism by which this inflammatory disease leads to cataract is not known, the potential of an immune cell-driven mechanism could explain why cataracts often develop in patients with uveitis and diabetes. The clinical link between uveitis and cataract, together with our finding that immune cells associate with the lens capsule in response to ocular trauma, raised the possibility that immune cells are targeted to the lens capsule in uveitis and that they can infiltrate the lens.

In this study we have investigated whether the inflammation seen in uveitis leads to the association of immune cells with the lens capsule using a well-established autoimmune disease model, experimental autoimmune uveitis (EAU).[29] This induced autoimmune disease results from subcutaneous immunization of C57BL/6J mice in their thighs and at the base of their tails with a uveitogenic epitope of the interphotoreceptor retinoid binding protein (hIRBP651-670).[30] The neural retina, normally protected by the blood-retinal barrier,[31–33] is targeted in EAU, with histopathological scoring of uveitis based on the extent of immune cell infiltration of the retina and the level of retinal damage.[29] EAU disrupts the cytoarchitecture of the retina with varying degrees of impact on the photoreceptor layer. In addition to this region of significant impact in the posterior chamber of the eye, EAU also causes inflammation in the anterior chamber, including immune cell infiltration of the ciliary body and the iris.[34] While cataract is reported among the ocular outcomes of uveitis, including in susceptible mouse models of EAU,[35] there is little understanding of the mechanisms that lead to lens pathologies in uveitis, including whether the lens is affected by immune cells directly or by the cytokines that they secrete. Our approach, which uses both high-resolution confocal microscopy and scanning electron microscopy (SEM) analyses, revealed that the inflammation that occurs in

the eyes of mice with EAU results in immune cells becoming closely linked to all surfaces of the lens capsule; anterior, equatorial, and posterior. The integration of immune cells with the lens capsule is maintained even after uveitic disease has peaked and inflammation begins to resolve. Many of the immune cells that associate with the surface of the lens in uveitis burrow within the lens capsule matrix and invade through it, with some infiltrating lens tissue, providing a possible explanation for inflammatory-mediated lens pathologies.

2 | MATERIALS AND METHODS

2.1 | Animals

Animal studies performed were approved by both George Washington University's Medical Center Institutional Animal Care and Use Committee (IACUC) and Thomas Jefferson University's IACUC. The investigations comply with all relevant guidelines. The animal studies also comply with the Association for Research in Vision and Ophthalmology Statement for the Use of Animals in Ophthalmic and Vision Research. All studies were performed with C57BL/6J mice (Jax Labs).

2.2 | Induction of EAU, disease scoring, and numbers of animals for analysis

Induction of EAU by active immunization was performed as described previously.[30] Briefly, C57BL/6J mice (Jax Labs) were immunized subcutaneously with 150 mg IRBP651-670 peptide (sequence LAQGAYRTAVDLESLASQLT), that was emulsified in an equal volume of Complete Freund's Adjuvant containing 2.5 mg/ml *M. tuberculosis*. These mice also received an intraperitoneal injection of 1.0 mg *Bordetella* pertussis toxin (Sigma-Aldrich, St. Louis, MO) on the day of immunization as reported previously.[30] Clinical EAU evaluation was performed by fundus examination using a scale of 0–4 that is based on the severity of inflammation.[29,36] Clinical scoring for these studies was performed at days 10, 12, 14, and 17 after disease was initiated (Figure S1). Consistent with previous findings,[30,37] disease severity peaked at D14. A minimum of three mice were used for each day post-induction of uveitis examined—D14, D19 and D26. One eye per mouse was used for immunofluorescent/confocal analysis, the other for SEM analysis. For the immunolocalization/confocal imaging studies whole eyes were enucleated and prepared for cryosectioning; for SEM analysis lenses were isolated from the enucleated eyes.

2.3 | Immunofluorescence

Immunolabeling studies were performed as described previously.[24] Briefly, whole mouse eyes removed immediately following euthanasia were fixed overnight at 4°C in 3.7% paraformaldehyde, washed in PBS, cryoprotected (30% sucrose in DPBS [2.7 mM KCl, 1.5 mM KH_2PO_4, 137.9 mM NaCl, 8.1 mM Na_2HPO_4–$7H_2O$, Corning]), frozen in Polyfreeze Tissue Freezing Media Red (Polyscience #25115) and cryosectioned using a Microm HM 550 Cryostat to produce 20 μm thick cryosections. Whole eye cryosections were permeabilized (0.5% Triton X100 in DPBS) for 1 h and incubated in block buffer (5% goat/donkey serum, 3% bovine serum albumin (BSA) in 0.5% Triton X-100-containing DPBS) for 2 h prior to overnight incubation at 37°C with primary antibody diluted in block buffer. Primary antibodies used in these studies included CD45 488 (Biolegend, 103122), CD45 594 (Biolegend, 103144), CD68 488 (Biolegend, 137012), GR1 594 (Ly-6G/Ly-6C, Biolegend, 108448), microfibril associated protein-1 (MAGP1; Santa Cruz, sc-50084), Perlecan (Santa Cruz, sc-33707), and TER-119 (Biolegend, 116218). Following washing, the sections were incubated for 1 h with an appropriate fluorescent-tagged secondary antibody (Jackson ImmunoResearch Laboratories) diluted in block buffer that included Alexa Fluor 488 donkey anti-goat #705-545-147, Alexa Fluor donkey anti-rat #712-545-153, Alexa Fluor 594 donkey anti-rat #712-585-153, and Alexa Fluor 594 goat anti-rat #112-585-167. F-actin was labeled with either Alexa Fluor 647 phalloidin (A22287, Invitrogen) or Alexa Fluor 594 phalloidin (A12381, Invitrogen), and nuclei labeled with DAPI (Biolegend, 422801) during the incubation with secondary antibody. The immunolabeled whole eye sections were mounted using ProLong Diamond Antifade Mountant (Invitrogen, P36970) and coverslipped with Fisher Scientific's Premium Cover Glass.

2.4 | Confocal image analysis

Fluorescent-labeled whole eye sections were imaged with the Zeiss LSM800 confocal microscope system which includes a 3PMT System, an URGB laser module with 4 laser Lines: 405, 488, 561, and 640, and a Zeiss Axio Imager Z2 microscope with a motorized XY scanning stage. Images were acquired in different regions of the eye with the Zeiss Plan-Apochromat 40×/1.3 Oil DIC M27 (WD = 0.20 mm) UV-IR objective. The Zeiss confocal operates with Zen software. Confocal *z*-stacks were acquired with the Zeiss 40× Plan-Apochromat objective, consisting of single optical slices of 0.5 μm.

2.5 | Imaris 3D surface rendering image analytics

Imaris 3D surface rendering software is a voxel-based technique that avoids visual artifacts by using the hierarchical Vector-to-Closest-Point (VCP) representation, which improves surface approximation quality of grid-based representations.[38] Imaris 3D rendering was applied directly to the high-resolution *z*-stacks at the magnification that they were acquired as described previously.[39] The automatic algorithm is used as default with the shortest distance calculation checked. These studies used the Imaris default smoothing factor, which doubles the voxel size, and the number of voxels Img = 1 default filter, after which step the algorithm is complete. The completed 3D surface rendering is accurate at arbitrary zoom-ins from a VCP grid, making it possible to zoom in without losing resolution. Therefore, Imaris creates the 3D surface structure at the magnification that the image was acquired, with voxel technology making it possible to enlarge the created surface rendering to view at higher zooms without compromising the original created 3D surface structure image.

2.6 | Scanning electron microscopy

For SEM analysis lenses were isolated from the eyes of normal mice and mice with EAU and the vitreous gently removed from the lenses prior to fixation in sodium cacodylate buffer containing 2.5% of glutaraldehyde and 1% of paraformaldehyde. Three control and 6 uveitic lenses were used per time point analyzed. The samples were rinsed and then postfixed in 1% osmium tetroxide. Serial dehydration in ethyl alcohol was followed by critical point drying (Autosamdri-931, Tousimis, Rockville, MD, USA). A thin layer of gold was sputtered onto the surface of the samples (Cressington 208HR, Ted Pella Inc, Redding, CA, USA) before imaging them in the FEI Teneo LV Scanning Electron Microscope (Thermo Fisher, Hillsboro, OR, USA). Imaging conditions were 2.0 KV with a working distance of 8.7 mm using the Everhart Thornley detector.

3 | RESULTS

3.1 | Immune cell distribution in regions of the eye surrounding the lens in the EAU model

The distribution of immune cells in the microenvironments surrounding the lens was examined by high-resolution confocal microscopy imaging at D14, D19, and D26 post-immunization of C57BL/6J mice with the uveitogenic hIRBP651-670 epitope. In this uveitis model, disease peaks at D14 with immune resolution in progress by D26.[30,37,40] The evaluation of disease severity post-induction of EAU by fundus examination as used in our study showed D14 as the height of posterior eye disease (Figure S1). Whole eye cryosections were immunolabeled for the common immune cell antigens CD45 or β2 integrin. CD45 is a transmembrane receptor-like protein-tyrosine phosphatase and one of the most abundant immune cell surface proteins.[41] β2 integrin/CD18 is an immune cell-specific integrin that mediates immune cell migration and infiltration of tissues.[42] In order to examine immune cell association with the ciliary zonules, the zonule fibrils were immunolabeled for MAGP1, an extracellular matrix protein that binds to fibrillin, the backbone of the zonule fibrils.[43] The sections were also labeled for F-actin and nuclei. Confocal microscopy *z*-stacks were collected in the aqueous humor (anterior chamber of the eye), along the ciliary zonules (the tendon-like fibrils that separate the anterior and posterior chambers and link the lens at its equatorial plane to the ciliary body), and across the vitreous humor (posterior chamber of the eye), as identified in the schematics (Figures 1, D19 and S2–S4). Data for D19 are presented in Figure 1 both as single optical planes from the *z*-stack, and as 3D surface structure renderings that were created from the *z*-stacks using Imaris advanced image analysis software. The results obtained at D19 are compared to those obtained at D14 and D26 in Figures S2–S4.

While EAU is an autoimmune disease that targets the neural retina, immune cells also populate the anterior segment, including the aqueous humor.[44] Immunolabeling studies show the presence of CD45+ immune cells throughout the aqueous humor at both D14 (Figure S2B) and D19 (Figures 1B and S2C), with some immune cells still detected in this region of the eye at D26 (Figure S2D). 3D surface renderings highlight the morphology of the immune cells in the aqueous humor and their tendency to aggregate in large clusters (Figures 1C and S2E–J). No CD45+ immune cells were detected in the aqueous or vitreous humors of naïve C57BL/6J mouse eyes (Figure S5).

The ciliary body is a vascularized region of the eye that, together with the iris and choroid, comprise the uvea. The non-pigmented ciliary epithelial cells that line the surface of its ciliary processes secrete the aqueous humor[45] and produce and maintain the ciliary zonule fibrils that link the ciliary body to the lens,[46] integrating with the lens capsule.[39] Our previous studies show that immune cells travel along these avascular fibrils to gain access to the lens.[24] In the eyes of mice with EAU, CD45+ immune cells are highly localized along the MAGP1-rich ciliary zonule fibrils at all timepoints examined, D14 (Figure S2L,O), D19 (Figures 1E,F and S2M,P) and D26 (Figure S2N,Q). 3D surface renderings of a selected region of the zonules (inserts,

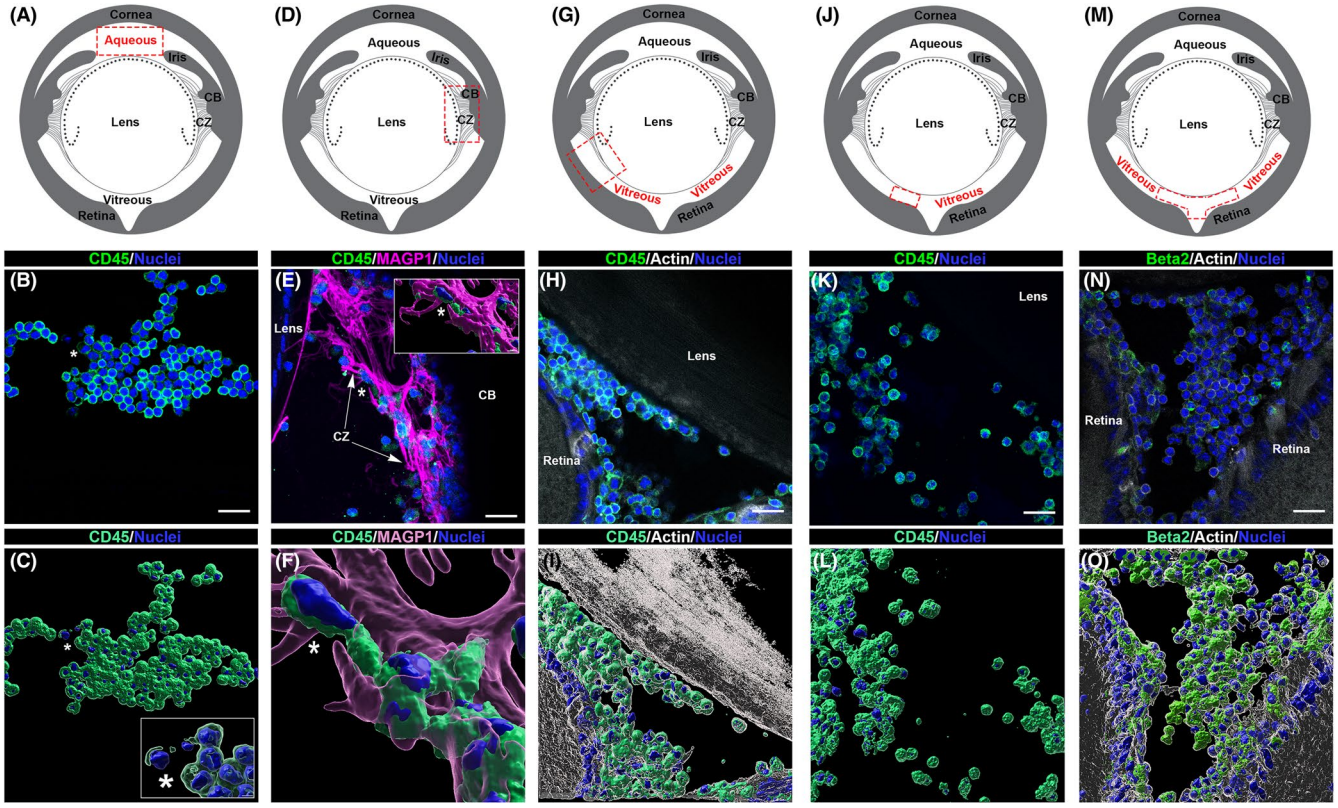

FIGURE 1 Inflammatory cells populate the environments surrounding the lens in EAU. Whole eye cryosections at D19 post-induction of uveitis were imaged by confocal microscopy following immunolabeling immune cells for CD45 or β2 integrin. Sections were co-labeled for nuclei and F-actin and ciliary zonules detected by labeling for MAGP1. *Z*-stacks were collected in the regions of the eye indicated in the diagrams including the aqueous humor (A–C), the ciliary zonules (D–F), the vitreous humor just beneath the zonules (G–I), a region of the vitreous mid-way between the zonules and the posterior-most aspect of the eye, and the posterior vitreous humor just adjacent to the retina (M–O). Images are shown as both a single 0.5 μm optical plane (B, E, H, K, and N) and the respective 3D surface renderings (C, F, I, L, and O). CD45 was rendered transparent in the inset in (C). The inset in E is a 3D surface structure of the region noted by an asterisk, which is shown zoomed-in with perlecan rendered transparent in F. CB, ciliary body; CZ, ciliary zonules. Mag bar 20 μm (B, C, E, H, I, K, L, N, and O), 5 μm (E insert, F), and 2 μm (C insert). The data presented represents at least 3 independent studies

Figures 1E and S2L–N), which are also zoomed in with MAGP1 rendered transparent (Figures 1F and S2O–Q), reveal the close association between these immune cells and the ciliary zonule fibrils. The density of immune cells associated with zonule fibrils in uveitis is much greater than has been observed in normal mouse eyes or in the response to corneal wounding.[24] These findings suggest that immune cells traveling across the ciliary zonules from the ciliary body are a principal source of immune cells that become associated with the equatorial lens capsule in EAU.

It has been shown that there is a high concentration of immune cells in the vitreous humor of mice with EAU, especially in the area juxtaposed to the inner limiting membrane of the retina.[40,47,48] In this study, we performed confocal imaging of immune cells in mice with EAU in three distinct regions of the vitreous with relevance to the lens at D14 (Figures S3 and S4), D19 (Figures 1G–O and S3, S4), and D26 (Figures S3 and S4) including: (1) just below the zonule fibrils where the lens and retina are closely apposed (Figures 1H,I and S3B–G); (2) the region just posterior to that imaged in (1) (Figures 1K,L and S3I–N); and (3) the most posterior region of the vitreous (Figures 1N,O and S4B–G). As expected, there were high concentrations of immune cells throughout the vitreous at days 14 and 19, often present in clusters, with immune cell prevalence in this region of the eye appearing lower by D26.

3.2 | Inflammation associated with uveitis leads to immune cells closely associating with the lens capsule

While many studies have investigated the infiltration of the neural retina by immune cells in the eyes of mice with EAU,[40,47,48] the impact of autoimmune inflammation on the lens, including whether lens immune privilege is abrogated, had not been previously assessed. We performed high resolution confocal microscopy imaging for immune

cells along 5 distinct regions of the lens capsule in whole eye cryosections at D14, D19, and D26 following labeling for CD45, F-actin and nuclei (Figure 2). Single optical planes are presented of confocal *z*-stacks acquired along (1) the anterior lens capsule where it faces the aqueous humor (Figure 2A–D), (2) the lens capsule at the border of its anterior and equatorial aspects (Figure 2E–H), (3) the lens equatorial capsule where it links to the ciliary zonules (Figure 2I–L), (4) the lens capsule at the border between its equatorial and posterior aspects (Figure 2M–P), and (5) the posterior lens capsule where it faces the vitreous humor (Figure 2Q–T).

We discovered that by D14, the height of uveitis, many immune cells had adhered to the lens capsule, most highly along its equatorial and posterior surfaces (Figure 2J,N,R). Quantification of these immunolocalization results, counting only those CD45+ cells that are in direct contact with the capsule surface, confirmed that at D14 there are significantly lower levels of immune cells associated with the anterior lens capsule than the posterior capsule (Figure 3B). This quantitative analysis provided the number of immune cells associated with the anterior, equatorial and posterior regions of the lens capsule relative to the immune cell burden in the aqueous and vitreous humors, providing an anatomical distribution of immune cells. Application of this quantitative approach to each time point in this study, D14, D19 and D26 after induction of EAU, showed that disease severity peaked at D14, consistent with fundus examination scores (Figure S1). At D14, there were fewer immune cells in the aqueous humor, as well as along the anterior and equatorial lens capsule surfaces, than were present along the surface of the posterior lens capsule and in the vitreous (Figure 3B). This finding is consistent with previous studies with this uveitis model that show the immune response begins in the retina and that disease severity peaks at this time.[30,37] By D19, immunolocalization analyses showed that the association of immune cells with the different regions of the lens capsule no longer suggested a posterior bias (Figure 2C,G,K,O,S), with quantification confirming that there were no significant differences in the number of immune cells between these sites (Figure 3C). The similarly high levels of immune cells along all regions of the lens capsule at D19 was consistent with increases in the number of immune cells populating the aqueous humor relative to the vitreous (Figure 3C). At D26 post-induction of EAU, when both inflammation and disease severity is known to be resolving,[30,37,40] immune cell prevalence is reduced with the vitreous retaining higher levels of immune cells than in the other regions assessed (Figure 3D). However, at D26 immune cells remained closely associated with the lens capsule (Figure 2D,H,L,P,T), and were present at similar levels along all regions of the lens capsule surface (Figure 3D). These results were unexpected and suggested that inflammatory cells of uveitic eyes can establish long-lasting, stable linkages with the lens capsule. No CD45+ immune cells were detected along the lens capsule of naïve C57BL/6J mice (Figure S6Aa–c), as we have shown previously in our studies of normal BALB/c mice.[24]

3.3 | Inflammation associated with EAU leads to association of T-cells, macrophages, and neutrophils with the lens capsule

While EAU is an induced T cell-mediated autoimmune disease,[29] neutrophils are also reported to infiltrate the retina,[49] and myeloid-derived suppressor cells (MDSC) to have an immunosuppressive role.[50] Therefore, we investigated the subset of immune cells that become linked to the lens capsule in the eyes of mice with EAU using antibodies to immune cell type-specific antigens at D14 (Figure S7), D19 (Figure 4), and D26 (Figure S8). For these studies, whole eye cryosections were immunolabelled using antibodies to the T cell antigen CD3 (Figures 4A,D,G, S7A,D,G and S8A,D,G), the macrophage/monocyte surface protein CD68 (Figures 4B,E,H, S7B,E,H and S8B,E,H), or the GR-1 antibody which recognizes the myeloid differentiation antigens LY6G/LY6C expressed on neutrophils and MDSC cells (Figures 4C,F,I, S7C,F,I and S8C,F,I). The sections were co-labeled for F-actin and nuclei. High resolution confocal images were acquired along the anterior lens capsule (Figures 4A–C, S7A–C and S8A–C), the equatorial lens capsule (Figures 4D–F, S7D–F and S8D–F) and the posterior lens capsule (Figures 4G–I, S7G–I and S8G–I). The results show a very high association of T-cells with the lens capsule, as well as a significant presence of both CD68+ and GR1+ immune cells. CD3+, CD68+, and GR1+ cells were linked to the lens capsule at the peak of uveitis (D14) and remained associated with the lens after resolution had begun (D26).

3.4 | Immune cells integrate with and invade the anterior lens capsule in uveitis

In our studies of the basement membrane capsule that surrounds the lens, perlecan has stood out as one if it's principal components.[39] As those studies showed a significant presence of perlecan in the outer depths of the lens capsule that extended to its superficial surfaces, we investigated the association and invasion of the lens capsule by immune cells in uveitic eyes by co-immunolabeling for CD45 and perlecan. As control for this study, cryosections of naïve C57BL/6J mice eyes (schematic, Figure 5Aa) were immunolabeled for perlecan, co-labeled for nuclei,

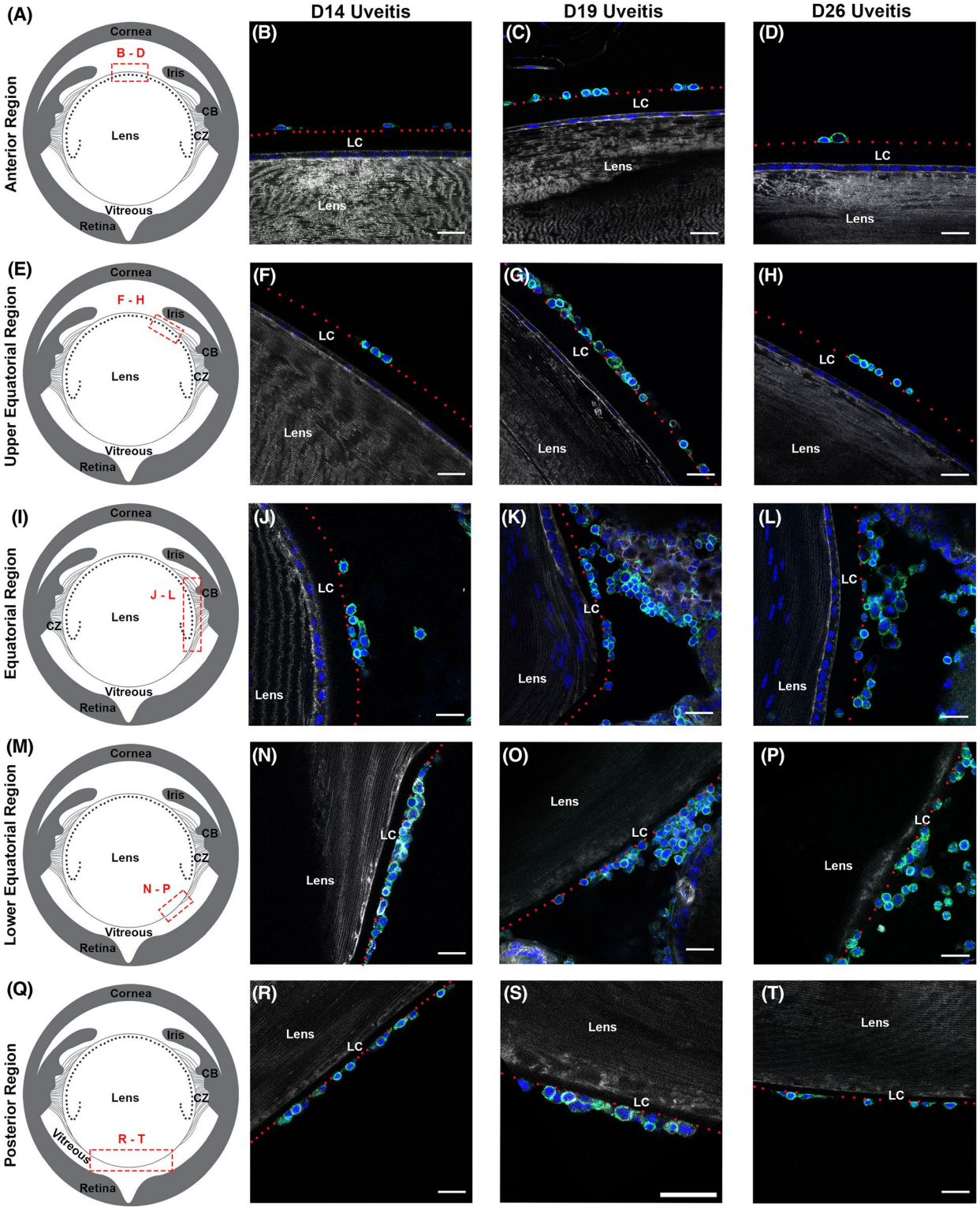

FIGURE 2 Immune cells become linked to the lens capsule in uveitic eyes. Whole eye cryosections from mice with EAU were co-labeled at D14, D19, and D26 for CD45 (green), F-actin (white) and nuclei (blue), and imaged by high resolution confocal microscopy. *Z*-stacks were collected in the following regions of the eye, as indicated in the diagrams: the anterior surface of the lens (A–D), the upper region of the lens equator at its border with the lens anterior zone (E–H), the lens equator (I–L), the lower region of the lens equator at its border with the lens posterior surface (M–P), and the posterior surface of the lens (Q–T). Red dotted lines identify the superficial surface of the lens basement membrane capsule (LC). CD45+ immune cells were detected along all surfaces of the lens capsule at D14, D19, and D26 post-induction of uveitis. CB, ciliary body. Mag bar 20 μm. The data presented represents at least 3 independent studies

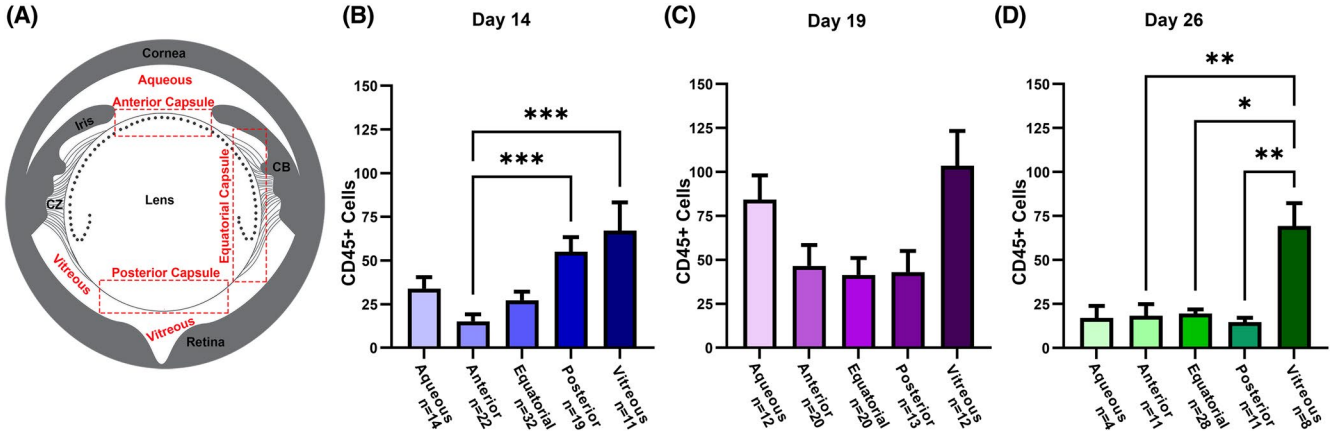

FIGURE 3 Quantification of the relative distribution of immune cells in different regions of uveitic eyes. Immune cell presence was quantified as indicated in the diagram (A) for the aqueous humor, the anterior, equatorial and posterior surfaces of the lens capsule, and the vitreous and compared at D14 (B), D19 (C), and D26 (D) post-induction of EAU. $*p < .02$, $**p < .005$, $***p < .001$

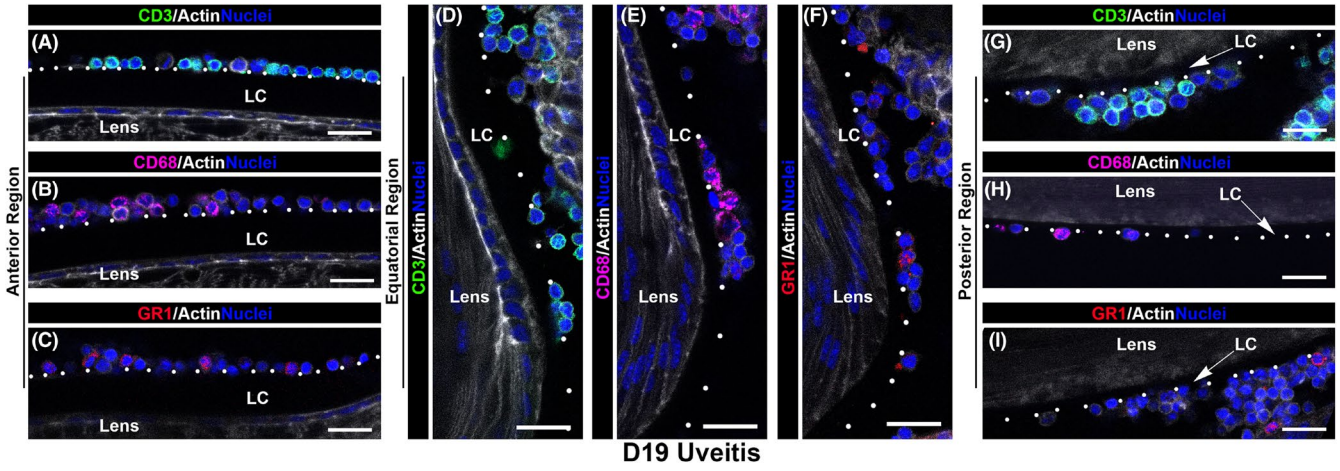

FIGURE 4 T cells, macrophages and Ly6G/Ly6C+ immune cells become associated with the lens surface in the eyes of mice with EAU. Whole eye cryosections from mice with EAU at D19 were immunolabeled for the T-cell antigen CD3 (A, D, and G), the macrophage antigen CD68 (B, E, and H), or the Ly6G/Ly6C antigen (GR-1) expressed by leukocytes and myeloid-derived suppressor cells (C, F, and I) and co-labeled for F-actin and nuclei. Single optical planes (0.5 μm) from confocal *z*-stacks acquired along the lens anterior, equatorial and posterior capsules show that T cells, macrophages and Ly6G/Ly6C+ immune cells associate with the lens capsule in uveitic eyes. White dotted lines identify the superficial surface of the lens basement membrane capsule (LC). Mag bar 20 μm. The data presented represents at least 3 independent studies

and imaged by confocal microscopy. Both a single optical plane of 0.5 μm (Figure 5Ba) and a 3D volumetric surface rendering (Figure 5Bb) are presented of a confocal *z*-stack acquired along the anterior capsule where it interfaces with the aqueous humor in these normal mice. The 3D image is rotated to visualize the anterior capsule's superficial surface face on, showing that it is relatively smooth, lacking pits or holes. This study also shows that the preparation of whole eye cryosections maintains the normal properties of the lens capsule, with no evidence of mechanical deformation.

The association of immune cells with the anterior lens capsule in uveitic eyes was analyzed in whole eye cryosections from mice with EAU at D14, D19 and D26 following co-labeling for perlecan, CD45 and nuclei (Figure 5). Confocal *z*-stacks were acquired at the interface of the anterior lens capsule and the aqueous humor. Single optical planes (0.5 μm) from the acquired *z*-stacks show that immune cells become integrated with the anterior lens capsule of uveitic eyes (Figure 5Ca,Da–c,Ea), sometimes moving completely across the capsule and positioning themselves amongst the cells of the lens epithelium (Figure 5Ea, arrow). As they invade the basement membrane of the anterior lens capsule they create pits and holes in this perlecan-rich matrix, with the degradation of the capsule emphasized in images with only the perlecan label displayed (Figure 5Dc,Eb). The digestion of the lens capsule by immune cells and the alterations of lens basement

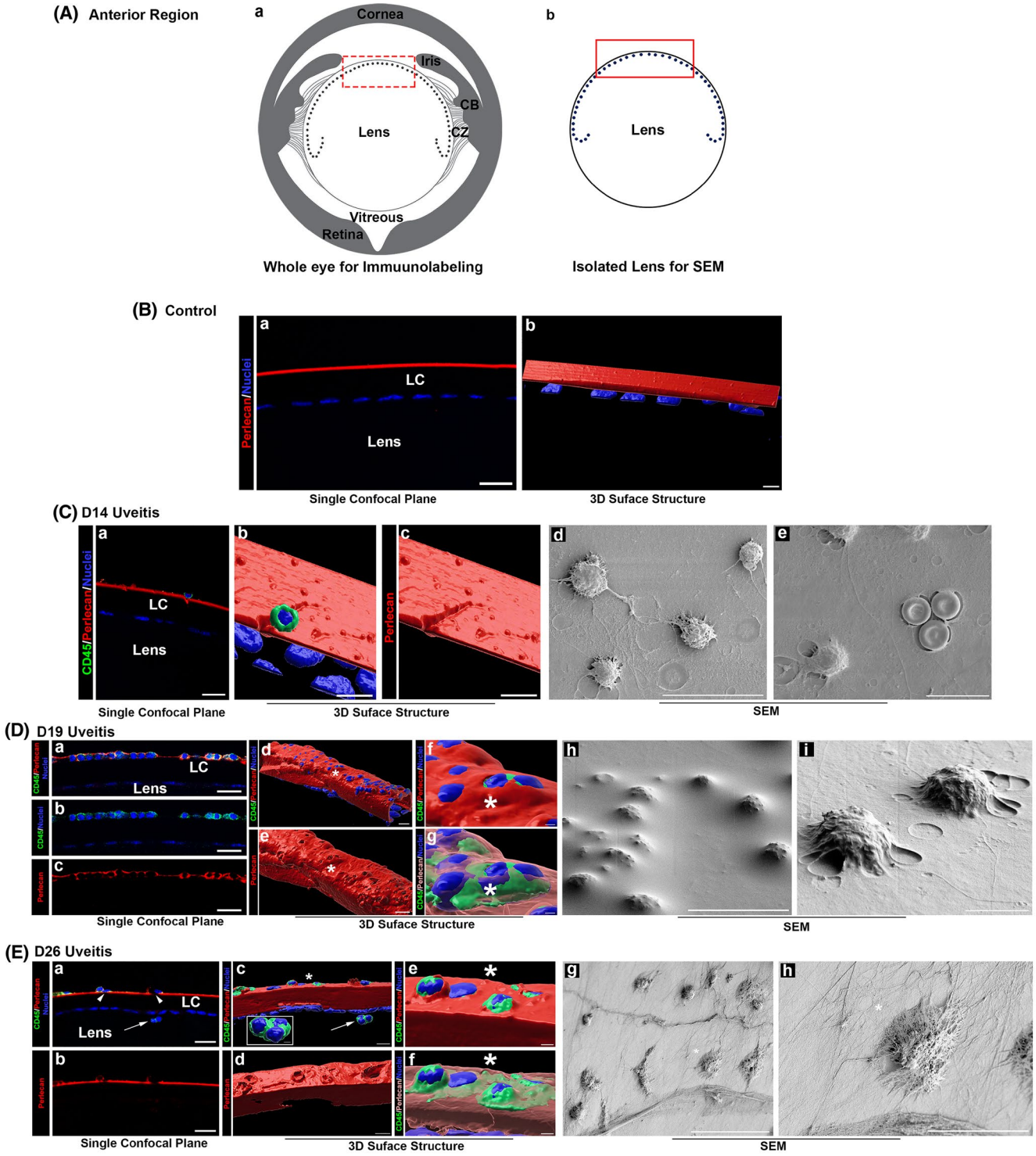

FIGURE 5 Legend on next page

membrane structure were further analyzed by creating 3D surface structure renderings, both with all fluorescent channels represented (CD45+ immune cells, perlecan and nuclei, Figure 5Cb,Dd,f,g,Ec,e,f) and with the perlecan channel alone (Figure 5Cc,De,Ed). The 3D renderings of just perlecan revealed the structure of the pits and holes in the anterior lens capsule in the spaces occupied by the invading immune cells, with indentations in the superficial surface of the lens anterior capsule at D14 becoming craters of significant size that envelop the immune cells by D19 (Figure 5Dd,e). By D26 some regions of the perlecan matrix have been completely digested away (Figure 5Ed).

A great advantage of the Imaris 3D rendering software is its use of voxel technology, which makes it possible

FIGURE 5 Immune cells induced in the eyes of mice with EAU become integrated with and migrate within the matrix of the anterior lens basement membrane capsule. Confocal *z*-stacks of whole eye cryosections of normal (B) and uveitic eyes at D14 (C), D19 (D), and D26 (E), were acquired along the lens anterior capsule, as indicated in the schematic (Aa). Normal eyes were co-labeled for perlecan and nuclei, uveitic eyes for CD45, perlecan and nuclei. Images are presented either as single 0.5 μm optical planes (Ba; Ca; Da–c; Ea,b) or 3D surface renderings (Bb; Cb,c; Dd–g; Ec–f) of the acquired *z*-stacks. The 3D surface renderings showing the integration of immune cells with the lens capsule at D14 (Cb), D19 (Dd) and D26 (Ec) were also created for the perlecan label alone (Cc, De, Ed, respectively) to show the impact of the immune cells on the degradation of the perlecan matrix. Zoomed-in views at D19 (Df) and D26 (Ee) are also shown with perlecan rendered transparent (Dg and Ef), which reveals the highly migratory morphology of the CD45+ immune cells as they burrow within the anterior lens capsule and the morphology and position of the CD45+ immune cells that have located within the lens capsule. The single optical plane of a uveitic eye at D26 (Ea) shows regions of the perlecan matrix that have been removed by the immune cells (arrowheads), and immune cells that have migrated across the lens capsule and come to reside amongst the cells of the lens anterior epithelium (arrow). SEM images acquired along the anterior surface (schematic, Ab) of lenses isolated from uveitic eyes at D14 (Cd,e), D19 (Dh,i), and D26 (Eg,h) provide a unique view of the morphology of the immune cells associated with the anterior capsule and their movement within the capsule matrix. Mag bars: 50 μm (Eg), 20 μm (Ba,b; Ca,d; Da,b,c,h; Ea,b,h), 10 μm (Cb,c,e; Dd,e; Ec,d), 5 μm (Di), 3 μm (Ee,f), 2 μm (Df,g). The data presented represents at least 3 independent studies

to enlarge images without compromising the 3D image created at the magnification at which the *z*-stack was acquired.[38] This technology provided the opportunity for a close examination of the integration of immune cells with the anterior lens capsule in uveitic eyes and to determine their morphology as they invade within this matrix structure. This objective was accomplished by first zooming in on the 3D surface structures (Figure 5Df,Ee), and then rendering the perlecan label transparent (Figure 5Dg,Ef), revealing the cells within the perlecan matrix. This analytical approach showed that in uveitic eyes immune cells are burrowed in just below the surface of the anterior lens basement membrane capsule and that these cells have a flattened morphology with lamellipodial leading edges that are characteristic of migrating, invading cells. Immune cells express integrins that give them the ability to adhere to and migrate across the lens capsule including the immune cell specific β2 integrins, α2β1 integrin, and α6β1/α6β4 integrins,[42,51,52] as well as secrete proteases that digest basement membrane proteins such as those that comprise the lens capsule including matrix metalloproteinases (MMPs) and cathepsin.[53–56]

Scanning EM studies of lenses isolated from uveitic eyes at D14, D19, and D26 (schematic, Figure 5Ab) provide a unique view of the immune cells as they adhere to and invade within the anterior surface of the lens capsule. SEM performed at D14 shows that many of these immune cells have extended dendritic-like processes along the surface of the anterior lens capsule (Figure 5Cd), some with the lamellipodia and trailing edges characteristic of migratory cells (Figure 5Ce). The SEM images also revealed pits or craters along the capsule surface that appear to represent areas where immune cells had begun to integrate with the lens capsule and had either migrated to another spot or been removed during sample preparation (Figure 5Cd). In addition, there were cells with a dimpled appearance (Figure 5Ce), whose morphology is suggestive of mouse erythroid cells. However, immunolabeling of whole eye cryosections for the erythroid marker TER-119 failed to demonstrate the presence of TER-119+ cells along the surface of the lens (Figure S6Ba). This finding suggested that the dimpled cells are immune cells actively burrowing into the capsule surface, a morphology consistent with the 3D surface structure rendering of a CD45+ immune cell at D14 shown in Figure 5Cb. At D19, SEM imaging showed that many immune cells appeared to become localized underneath the surface of the anterior capsule (Figure 5Dh), while others remaining closer to the capsule's superficial surface were covered with a thin layer of matrix-like material and surrounded by a cratered capsule surface (Figure 5Di). At D26, the SEM images show that at the anterior capsule surface immune cells were integrated within the capsule surface and covered by a fibrillar, net-like substance (Figure 5Eg,h). The area along the anterior capsule from which these SEM images were obtained also are provided at low magnifications alongside these higher magnification views in Figures S9A,Ai,Aii,B,Bi,Bii (D14), S10A,Ai,B,Bi (D19), and S11A,Ai (D26).

3.5 | In uveitic eyes immune cells invade the equatorial lens capsule just adjacent to the ciliary zonules

The lens equatorial capsule is a unique matrix environment with two laminin/perlecan-rich basement membrane lamella.[39] The more prominent one is located within the outer regions of the thick equatorial capsule and is an integration site for the ciliary zonules.[24,39] As a control for our studies of the association of immune cells with the equatorial lens capsule in uveitic eyes, we examined the surface structure of this region of the capsule in cryosections of naïve C57BL/6J mouse eyes (schematic,

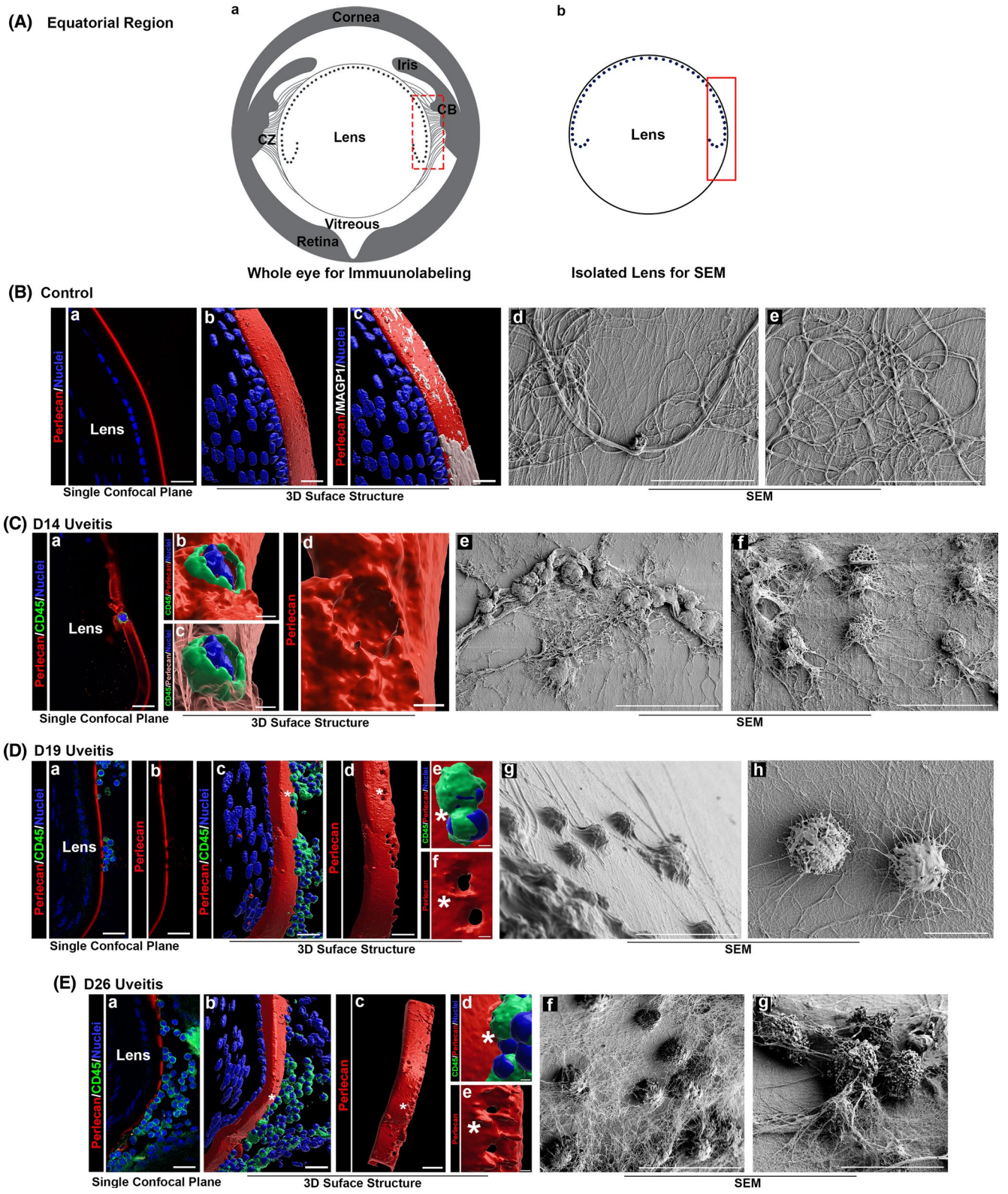

FIGURE 6 Legend on next page

Figure 6Aa), which were co-labeled for perlecan, the ciliary zonule protein MAGP1, and nuclei. Confocal microscopy *z*-stacks were collected, and the perlecan/nuclei labels are shown together as both a single optical plane of 0.5 μm (Figure 6Ba) and a 3D volumetric surface rendering that is rotated to view the equatorial capsule's superficial surface, revealing a linear structural patterning on an otherwise smooth external facing surface (Figure 6Bb). Including the MAGP1 channel in this 3D surface rendering shows the MAGP1+ zonule fibers extended anteriorly along the

FIGURE 6 Immune cells induced in the eyes of mice with EAU rapidly become integrated with and migrate within the lens equatorial capsule. Confocal *z*-stacks of whole eye cryosections of normal (B) and uveitic eyes at D14 (C), D19 (D), and D26 (E), were acquired at the equatorial zone of the lens capsule, as indicated in the schematic (Aa). Normal eyes were co-labeled for perlecan, nuclei, and MAGP1, uveitic eyes for CD45, perlecan and nuclei. Images are presented either as single 0.5 μm optical planes (Ba; Ca; Da,b; Ea) or 3D surface renderings (Bb,c; Cb-d; Dc-f; Eb-e) of the acquired *z*-stacks. The 3D surface renderings created to view immune cells association with the lens capsule at D14 (Cb), D19 (Dc,e) and D26 (Eb,d) were also created for the perlecan label alone (Cd; Dd,f; Ec,e, respectively), revealing the degradation and removal of the perlecan matrix by the immune cells as they invade the lens capsule over time. The zoomed-in view at D14 (Cb) is also shown with perlecan rendered transparent (Cc) to reveal this immune cell burrowing into the perlecan matrix. SEM images are presented of ciliary zonules on the surface of the equatorial capsule of lenses (schematic, Ab) isolated from normal eyes (Bd,e), and of the immune cells associated with the surface of the equatorial lens capsule at D14 (Ce,f), D19 (Dg,h), and D26 (Ef,g) post-induction of uveitis. These images highlight the rounded morphology of the immune cells associated with the equatorial capsule and the fibrillar structures that link them to the capsule surface. Mag bars: 40 μm (Ce), 30 μm (Cf), 20 μm (Ba–e; Ca; Da–d; Dg; Ea–c; Eg; Eh), 5 μm (Dh), 3 μm (Cb–d), 2 μm (De,f; Ed,e). The data presented represents at least 3 independent studies

surface of the lens from their site of contact and integration at the lens equator (Figure 6Bc). SEM imaging of the equatorial surface of lenses from naïve C57BL/6J mice details the organization and distribution of the lens-associated ciliary zonule fibrils and the absence of any immune cells (Figure 6Bd,e), as shown in our previous findings.[24] In addition, the SEM imaging of naïve C57BL/6J mice provide evidence of the absence of pits and holes in the normal capsule surface as well as the absence of any amorphous material associated with the lens capsule.

Our studies above show that the ciliary zonules in the eyes of mice with EAU are populated by many immune cells from D14 through D26 (Figures 1E,F and S2L–Q), and suggest that the zonule fibrils are a path for the immune cells that come to associate with the surface of the lens equatorial capsule (Figure 1E). To investigate the degree of integration and stabilization of the immune cells that locate to the lens equatorial capsule in uveitic eyes, whole eye cryosections were co-labeled for CD45, perlecan, and nuclei, and confocal microscopy *z*-stacks acquired of the region of the equatorial capsule juxtaposed to the ciliary zonule fibrils. Single optical planes of the *z*-stacks (0.5 μm) at D14, D19 and D26 show that these immune cells, most with a rounded morphology, are integrated with the surface of the perlecan-rich equatorial basement membrane capsule by D14 (Figure 6Ca), and that over time these immune cells cause significant degradation of the perlecan matrix as they invade through this region of the capsule (D19 and D26, Figure 6Da,b,Ea, respectively). Zoomed in views of a 3D surface rendering created of the immune cell that appears in the single optical plane at D14 shows early stages in the integration of these cells with the perlecan matrix at the lens equatorial surface (Figure 6Cb). Rendering perlecan transparent in this 3D image reveals the portion of this cell that is burrowing within the lens capsule (Figure 6Cc). A further enlargement of this same region for perlecan alone, created without the immune cell channel, shows how the cell has degraded the perlecan-rich capsule as it integrates within it (Figure 6Cd). 3D surface renderings of whole eye cryosections co-labeled for CD45, perlecan, and nuclei at D19 (Figure 6Dc) and D26 (Figure 6Eb) show that many immune cells are still located near the lens capsule equatorial surface, and retain their rounded morphology while they degrade the perlecan matrix and invade into the capsule. The impact of this invasion on the perlecan-rich capsule is revealed when these 3D renderings are created of the perlecan channel alone (Figure 6Dd,Ec). These images show that the immune cells invading the surface of the equatorial lens capsule create pits and holes in the perlecan matrix, which are shown in detail with zoomed in views in Figure 6De,f,Ed,e. While the integration of the immune cells with the equatorial surface of the lens has similar impact on the capsule to those invading at its anterior aspects, the morphology of these cells as they invade the capsule matrix in these two regions of the lens is distinct.

SEM images of the surface of lenses from mice with EAU (schematic Figure 6Ab) confirm the rounded morphology of the immune cells directly associated with the surface of the equatorial lens capsule. At D14 these immune cells were shown to be entwined with the ciliary zonules that are located along the surface of the equatorial capsule (Figure 6Ce,f). By D19 many of the immune cells are well-integrated within the surface of the capsule matrix (Figure 6Dg), while others that remain along the capsule surface are still associated with ciliary zonules (Figure 6Dh). SEM images acquired at D26 show that by this later stage in the eyes of mice with EAU many of the immune cells exposed on the surface of the lens equatorial capsule are covered with fibrillar-like nets (Figure 6Ef,g). The area along the equatorial capsule from which these SEM images were obtained are provided at low magnification alongside these higher magnification views in Figures S9C,Ci,D,Di,E,Ei (D14), S10C,Ci,D,Di,E,Ei (D19), and S11B,Bi,C,Ci,D,Di,E,Ei (D26).

3.6 | Immune cell interactions with the vitreous-facing posterior lens capsule in the eyes of mice with EAU

The primary inflammatory reaction in EAU occurs in the posterior eye chamber with immune cells infiltrating and causing damage to the retina.[29,30,57] Therefore, while our results show that immune cells are also recruited to the anterior and equatorial regions of the lens capsule in EAU, their impact on the posterior capsule has particular relevance to this model. Our control studies of the posterior lens capsule where it interfaces with the vitreous in whole eye cryosections (schematic, Figure 7Aa) from naïve C57BL/6J mice co-labeled for perlecan and nuclei show that perlecan is a major component of this region of the capsule (Figure 7Ba, single optical plane; Figures 7Bb, 3D volumetric surface rendering) and is not detected in the adjacent vitreous. Rotation of the 3D image to view the surface of the lens capsule face on, shows that the superficial surface of the posterior capsule in naïve mice is very smooth with no evidence of pits or holes (Figure 7Bc).

Confocal *z*-stacks acquired in this region of the posterior capsule in whole eye cryosections from mice with EAU at D14, D19 and D26 co-immunolabeled for CD45, perlecan, and nuclei are represented here as both 0.5 μm single optical planes (Figure 7Ca,Da,Ea) and 3D surface renderings (Figure 7Cb–g,Db–g,Eb–e). Analysis of uveitic eyes at D14 and D19 shows that the immune cells associated with the posterior capsule are primarily rounded and clustered together. They are sometimes linked to larger immune cell clusters that extend into the vitreous, suggesting that they have been recruited from the vitreous. 3D surface renderings of the posterior capsule region at D14, created with (Figure 7Cb) and without (Figure 7Cc) the CD45 and nuclear channels, show that the regions occupied by immune cells have created pits and small holes as they integrate with the posterior capsule's perlecan matrix. A closer view of this degradation of the posterior capsule by immune cells is shown by zooming in on this 3D surface rendering (Figure 7Cd–g). As occurs in other regions of the lens capsule, the degradation of the lens capsule matrix by the associated immune cells increases between D14 and D19, with numerous holes and craters created as immune cells invade the posterior capsule (Figure 7Db–g). Distinct from the equatorial zone at D19, immune cells that burrow into this capsule zone have a flattened morphology (Figure 7Df). By D26, as inflammation in the vitreous compartment is resolving, a population of immune cells remains closely associated with the surface of the posterior capsule (Figure 7Ea,b), most with a spread morphology and well-integrated with the perlecan matrix (Figure 7Eb,d). The degradation of the perlecan matrix at D26 by the posterior capsule associated immune cells is seen as the loss of perlecan under the cells in the single 0.5 μm optical plane (Figure 7Ea), with the structure of these degraded regions of the capsule shown in the 3D surface rendering of perlecan created in the absence of the associated immune cells (Figure 7Ec,e). The generally rough appearance of the superficial surface of the posterior capsule at D26 in regions where no immune cells were detected suggests that remodeling of this matrix was executed by immune cells that had previously populated this region of the capsule.

SEM images were acquired along the surface of the posterior lens capsule following removal of lenses from uveitic eyes at D14, D19 and D26 (schematic, Figure 7Ab). At D14 a large number of immune cells with a rounded morphology are closely associated with the posterior capsule (Figure 7Ch,i), many of which are covered and linked together by a fibrillar network (Figure 7Ch). These fibrils often appear to provide a supportive covering that links these immune cells to the surface of the posterior capsule (Figure 7Ci). By D19, while many of these immune cells remain close to the surface of the lens, they also appear to have migrated within the posterior capsule matrix, covered with an amorphous substance that could be composed of extracellular matrix proteins (Figure 7Dh,i). SEM images of the posterior capsule of lenses isolated from D26 EAU eyes show that at this late stage following induction of uveitis there is a mix of immune cell morphologies, some rounded and others flattened and covered with an amorphous material (Figure 7Ef) or with fibrillar nets (Figure 7Eg). Cells with a dimpled appearance were sometimes detected. The region of the posterior capsule surface from which these SEM images are obtained are provided at low magnification alongside these higher magnification views in Figures S9F,Fi,Fii,G,Gi,Gii (D14), S10F,Fi (D19), and S11F,Fi,G,Gi (D26).

3.7 | Inflammatory cells in the eyes of mice with EAU infiltrate the lens

The studies above show that immune cells become integrated with the lens capsule by D14 and have degraded and invaded this matrix by D19 in mice with EAU. These findings demonstrate that the capsule is not a barrier to inflammatory cells and that immune privilege of the lens is abrogated in uveitic eyes. While many immune cells that associate with and become integrated with the lens capsule appear to remain within the capsule matrix, these cells also have the potential to infiltrate lens tissue. To examine this possibility and potential sites of immune cell localization in the lens

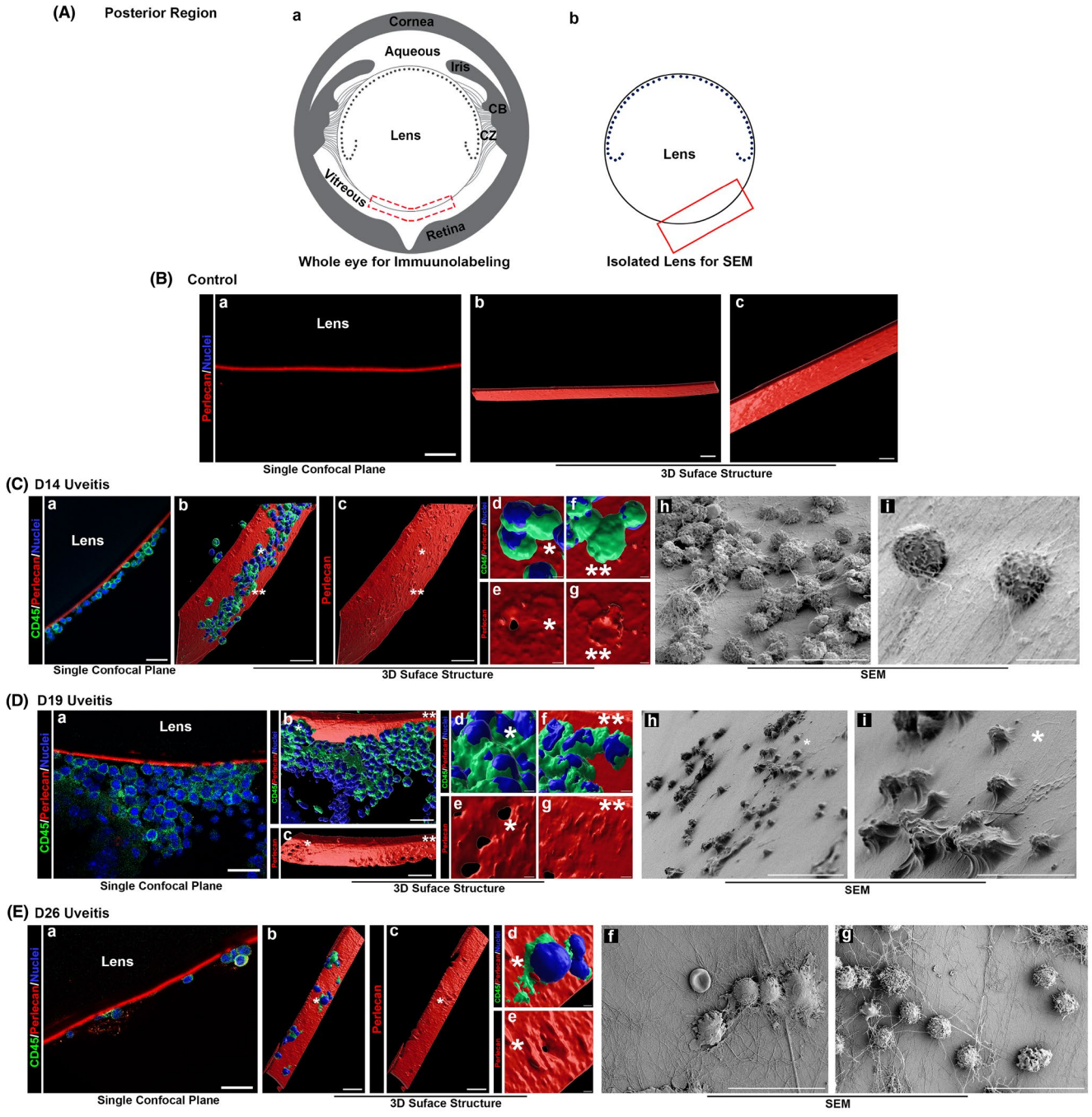

FIGURE 7 Immune cells induced in the eyes of mice with EAU become integrated with the lens posterior capsule. Confocal *z*-stacks of whole eye cryosections of normal (B) and uveitic eyes at D14 (C), D19 (D), and D26 (E), were acquired along the posterior the lens capsule, as indicated in the schematic (Aa). Normal eyes were co-labeled for perlecan and nuclei, uveitic eyes for CD45, perlecan and nuclei. Images are presented either as single 0.5 μm optical planes (Ba, Ca, Da, Ea) or 3D surface renderings (Bb,c; Cb-g; Db-g; Eb-e) of the acquired *z*-stacks. The 3D surface renderings created to view immune cells association with the lens capsule at D14 (Cb,d,f), D19 (Db,d,f) and D26 (Eb,d) were also created for the perlecan label alone (Cc,e,g; Dc,e,g; Ec,e, respectively), revealing the degradation and removal of the perlecan matrix by the immune cells as they integrate with and invade the lens capsule over time. SEM images presented of the immune cells associated with the posterior lens capsule (schematic, Ab) at D14 (Ch,i), D19 (Dh,i), and D26 (Ef,g) post-induction of uveitis highlight the rounded morphology of the immune cells associated with the posterior capsule and the fibrillar structures that link them to the capsule surface. Mag bars: 50 μm (Dh), 20 μm (Ba; Ca–c,h; Da–c,i; Ea–c,f,g), 10 μm (Bb), 5 μm (Ci), 3 μm (Df,g), 2 μm (Cd–g; Dd,e; Ed,e). The data presented represents at least 3 independent studies

after migrating across the lens capsule, confocal *z*-stacks were acquired of whole eye cryosections immunolabeled for immune cells using antibodies to both CD45 and β2 integrin. By D14, CD45+ immune cells that had become integrated with and invaded through the lens equatorial capsule were detected just adjacent to the

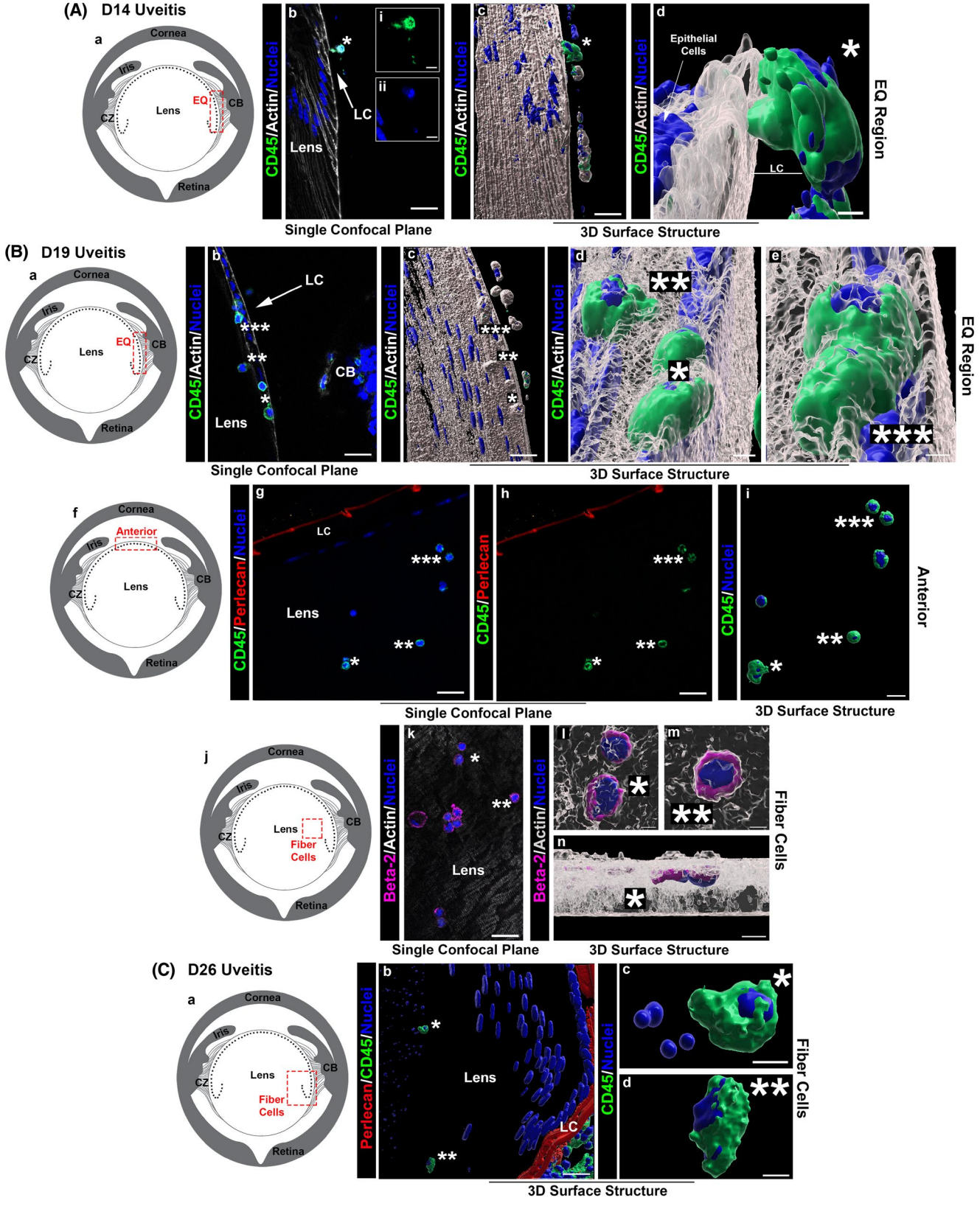

FIGURE 8 Legend on next page

lens epithelium, shown here as a single optical plane within the acquired *z*-stack (Figure 8Ab, 0.5 μm optical section at 9 μm within the cryosection), a 3D surface structure of this *z*-stack (Figure 8Ac), and a zoomed in view of the 3D image with F-actin rendered transparent (Figure 8Ad). By D19, immune cells had infiltrated this region of lens (Figure 8Bb, 0.5 μm optical section at 10 μm within the cryosection and 8Bc, 3D surface

FIGURE 8 Infiltration of the lens by immune cells in mice with EAU. Whole eye cryosections from mice with EAU were examined at (A) D14, (B) D19, and (C) D26 post-induction of uveitis for the presence of immune cells that had infiltrated the lens. Immune cells were detected by immunolabeling for either CD45 or β2 integrin and the sections co-labeled for nuclei. Sections were also labeled for either F-actin or perlecan. Confocal *z*-stacks were acquired in the region of the lens equatorial epithelium (Ab–d, Bb–e), the lens anterior zone (Bg–i), and the lens cortical fiber zone, a region between the equatorial epithelium and central fiber cells (Bk–n; Cb–d), as indicated in the diagrams. Images shown are either single 0.5 μm optical planes (Ab; Bb,g,h,k), 3D surface structures (Ac,d; Bc–e,i,l–n; Cb–d), or 3D surface structures in which F-actin is rendered transparent to highlight the presence of the immune cells within lens tissue (Ad; Bd,e,l–n). By D19 after induction of uveitis immune cells have crossed the lens anterior and equatorial capsules and infiltrated lens tissue. LC, lens capsule. Mag bars: 20 μm (Ab, Ac, Bb, Bc, Bg, Bh, Cb), 10 μm (Bi), 5 μm (Ab, inserts), 4 μm (Bn), 3 μm (Ad, Bd, Bl, Bm, Cc, Cd), 2 μm (Be). The data presented represents at least 3 independent studies

rendering of the *z*-stack). Zooming into this 3D image and rendering F-actin transparent shows that CD45+ immune cells had become localized among both the cells of the lens equatorial epithelium (Figure 8Be) and the adjacent nascent lens fiber cells (Figure 8Bd). By D19, immune cells had also infiltrated the anterior region of the lens. Here, in a 0.5 μm optical section located within the *z*-stack with perlecan and epithelial cell nuclei as references (Figure 8Bg,h), CD45+ immune cells are shown to have become located within the anterior aspects of the lens, their morphology highlighted in a 3D surface rendering (Figure 8Bi). At D19, some immune cells (β2 integrin+) had also infiltrated somewhat deeper within the lens, shown here in an example of immune cells located amongst lens fiber cells, their position suggesting that they had invaded the lens equatorial capsule (Figure 8Bk, 0.5 μm optical section at 6 μm within the cryosection). Zoomed in images of 3D surface structures are shown for a few of these cells with F-actin rendered transparent, with both face-on and side views provided (Figure 8Bl–n). Immune cells are still detected in this region of the lens at D26, shown here as a 3D surface structure with both perlecan and nuclei as references (Figure 8Cb) and with zoomed-in views highlighting immune cell morphology (Figure 8Cc-d) and their position adjacent to the condensed nuclei of differentiating lens fiber cells (Figure 8Cc). These results provide evidence that immune cells that invade the lens capsule in uveitic eyes infiltrate the lens and can persist as uveitis improves and inflammation resolves.

4 | DISCUSSION

The avascular properties of the eye are crucial to maintaining the transparency required for clear vision. As such, inflammatory cells that are activated and recruited to the eye in response to injury, trauma or pathological conditions must be tightly regulated, with the rapid resolution of the immune response key to preventing persistence of immune cells that can impair vision. The presence of inflammatory cells in the eye that occurs in uveitis or diabetes has been linked to immune cell infiltration of the retina, leading to significant tissue damage.[2,7–9] While there are clinical links between uveitis and the appearance of cataracts, and poor outcomes to cataract surgery leading to PCO in patients with uveitis,[12–18] it was not previously investigated whether in uveitic eyes there is immune cell infiltration of the lens that could lead to lens pathologies.

The cornea, lens, and retina are commonly known as sites of immune privilege, a property that is essential to maintaining transparency in the central light path of the eye. Immune privilege of the adult lens is primarily conferred by the absence of a closely associated vasculature. It was also believed that the basement membrane capsule surrounding the lens functioned as a barrier to immune cells in its microenvironment, conferring immune privilege. However, in studies of the corneal wounded eye it was discovered that surveillance of the lens by immune cells is induced and that these cells are able to invade into the lens capsule.[24] While it had been previously demonstrated that there is an adaptive immune response to lens dysgenesis in the presence of an intact lens capsule,[25] the cornea injury studies provided the first evidence of immune cells actively moving within the lens capsule.[24] These results suggested that inflammation occurring in the lens environment, as occurs in uveitis, could result in immune cells associating with and populating the lens. Now, in studies of mice with EAU we show for the first time that the inflammatory cells induced in this model of uveitis become linked in high numbers to the surface of the lens capsule, and importantly, that the association of immune cell types with the lens surface persists past the height of EAU induced inflammation. It is likely that these immune cell interactions with the lens capsule are dependent on the activation of integrins expressed on the surface of immune cells,[58,59] and that MMPs expressed by the immune cells are required for the integration of immune cells with the capsule surface and their continued migration through the lens basement membrane capsule.[60]

The types of immune cells that were associated with the lens capsule in uveitic eyes included CD3+ T cells, CD68+ macrophages, as well as Ly6G/Ly6C+ cells that

could include both neutrophils and MDSCs. In future studies, it will be interesting to determine whether MDSCs are among the immune cells linked to the lens surface in uveitic eyes, as this would suggest a potential role for lens-associated immune cells in modulating the inflammatory response and participating in immune resolution.[50] Our previous finding that Ly6G/Ly6C+ cells are among the immune cells that associate with the surface of the anterior lens capsule following corneal wounding[24] may also be an example of the extracellular matrix on the lens capsule surface functioning as a sink for immune cells with functions in suppressing inflammatory responses. Along this same line of thought is the likelihood that matrix proteins and matrix-derived peptides released by proteolytic degradation of the lens capsule as immune cells integrate within the lens capsule, such as matrikines, could also play a role in regulating the immune response. These matrikines could include bioactive molecules like endostatin and endorepellin with anti-angiogenic, anti-fibrotic, and immunomodulatory properties[61–65] that could hold a key to understanding maintenance/restoration of homeostasis in uveitis.

The stability of the association between the immune cells and the lens capsule in the eyes of mice with EAU led us to examine how the strength of this interaction is achieved. These studies revealed that the immune cells that had infiltrated into the uveitic eye and associated with the surface of the lens capsule became integrated with the capsule's basement membrane proteins. These studies also revealed that, over time, many of these immune cells migrate further within the lens capsule, digesting the perlecan matrix as they invade into the capsule matrix. SEM imaging provided further evidence of how eye infiltrating immune cells in uveitis associate with the surface of the lens capsule, and the unique properties of this interaction in different regions of the lens. Many of the immune cells associated with the anterior surface of the lens capsule surface had a migratory morphology, with both leading lamellipodial and trailing edges. In this capsule zone many of the associated immune cells become located just under the capsule surface. In contrast, most of the immune cells along the equatorial and posterior surfaces of the lens retained a rounded morphology and appeared trapped in nets, possibly matrix fibers, that cover the top surface of the immune cells and link them to the lens capsule surface.

While many of the capsule associated immune cells remain integrated within the lens capsule, often near the capsule's surface, our imaging studies revealed that immune cells also penetrated through the entire thickness of the lens capsule and infiltrated the lens, particularly in the anterior and equatorial regions of the lens. Immune cells were observed amongst the lens epithelial cells, the nascent, cortical fiber cells and even deeper into the fiber cell region. These immune cells persisted even as inflammation is resolving in these uveitic eyes. This discovery could have significant implications for understanding lens pathologies, including providing a potential mechanism by which uveitis promotes lens cataract. Infiltration of the lens by immune cells in uveitic eyes appears to occur primarily in the anterior and equatorial regions of the lens. This finding is likely to reflect the contribution of cytokines produced by lens epithelial cells, which line the anterior and equatorial capsules, but not the posterior lens capsule. The secretion of cytokines by epithelial cells that sense danger set up a cytokine gradient that signals immune cells to travel to these sites.[66,67] Also relevant to immune cell infiltration of the lens are previous studies that showed the potential for immune cells recruited to dysgenic lenses to acquire a myofibroblast phenotype.[25] Lens opacities associated with cataract have often been shown to be characterized by the presence of alpha smooth muscle actin-expressing cells and their production of collagen I, both hallmarks of fibrosis. Uveitis-linked cataractogenesis could also result from the impact of the physical attachment of immune cells on the lens, or be an indirect effect related to the chemokines produced by immune cells that have infiltrated the lens or by the immune cells in the environment surrounding the lens. In future investigations, it will be important to perform longer-term studies with the mouse EAU model focused on investigating the fate of the immune cells that populate the lens in uveitic eyes and their potential role in induction of cataractogenesis.

In our studies of the association of immune cells with the lens capsule surface in response to corneal wounding, immune cells localized specifically along the lens' anterior and equatorial surfaces, no immune cells were detected along the lens posterior surface. In contrast, in uveitis immune cells are present along all surfaces of the lens capsule, consistent with their population of the aqueous humor, the ciliary zonules, and the vitreous humor, which contact the lens anterior, equatorial and posterior capsule surfaces, respectively. The lens-associated immune cells could be sourced from all or just one of these regions of the eye. Interestingly, our confocal imaging studies show an even greater presence of immune cells along the ciliary zonule fibrils in uveitic eyes and along the equatorial lens capsule than we have had observed in the response to cornea wounding, emphasizing that the ciliary body and the zonules that link this tissue to the lens, are likely an important source of the immune cells that associate with the lens in uveitis.

The discoveries that the inflammation of the eye that occurs in uveitis leads to immune cells becoming highly linked to surface of the lens and that these immune cells become integrated with and then cross the lens basement

membrane capsule to populate the lens, show that immune privilege of the lens can be abrogated and opens many important new areas of research. Such studies suggest a novel perspective for understanding the clinical link between inflammation of the eye and cataractogenesis, particularly in autoimmune diseases like uveitis and diabetes, and may also have implications for lens pathologies associated with inflammation of the eye that occurs with aging. Another exciting area important to pursue is the possibility that a subset of immune cells that become associated with the lens in response to inflammation of the eye may play a regulatory role in immune resolution. The new findings we present in this study suggest that the lens, with its central position vis-à-vis most other tissues of the eye, may play previously unappreciated roles in regulating inflammation in the eye and could impact the progression of various eye pathologies.

ACKNOWLEDGEMENTS

This work was supported by a grant from the National Institute of Health, National Eye Institute, EY021784 to ASM and MAS. Scanning Electron Microscopy was done at the GWU Nanofabrication and Imaging Center directed by Anastas Popratiloff.

DISCLOSURES

The authors declare no competing interests.

AUTHOR CONTRIBUTIONS

JodiRae DeDreu performed research, analyzed data and wrote the paper including creating the figures for the paper, Sonali Pal-Ghosh, performed research for the paper; Mary J. Mattapallil performed research, providing the mice for the studies, and reviewed and edited the paper; Rachel R. Caspi developed the methodology and mice for the studies, and reviewed and edited the paper, Mary Ann Stepp designed the research, analyzed the data and wrote the paper, A. Sue Menko designed the research, analyzed the data and wrote the paper. All authors approved the final manuscript.

ORCID

Mary Ann Stepp https://orcid.org/0000-0001-5623-2538
A. Sue Menko https://orcid.org/0000-0002-7514-4696

REFERENCES

1. Streilein JW. Ocular immune privilege: the eye takes a dim but practical view of immunity and inflammation. *J Leukoc Biol*. 2003;74:179-185.
2. Perez VL, Caspi RR. Immune mechanisms in inflammatory and degenerative eye disease. *Trends Immunol*. 2015;36:354-363.
3. Rosenbaum JT, Rosenzweig HL, Smith JR, Martin TM, Planck SR. Uveitis secondary to bacterial products. *Ophthalmic Res*. 2008;40:165-168.
4. Sharma SM, Jackson D. Uveitis and spondyloarthropathies. *Best Pract Res Clin Rheumatol*. 2017;31:846-862.
5. Rosenzweig HL, Jann MM, Glant TT, et al. Activation of nucleotide oligomerization domain 2 exacerbates a murine model of proteoglycan-induced arthritis. *J Leukoc Biol*. 2009;85:711-718.
6. Kezic JM, Glant TT, Rosenbaum JT, Rosenzweig HL. Neutralization of IL-17 ameliorates uveitis but damages photoreceptors in a murine model of spondyloarthritis. *Arthritis Res Ther*. 2012;14:R18.
7. Mölzer C, Heissigerova J, Wilson HM, Kuffova L, Forrester JV. Immune privilege: the microbiome and uveitis. *Front Immunol*. 2020;11:608377.
8. Burkholder BM, Jabs DA. Uveitis for the non-ophthalmologist. *BMJ*. 2021;372:m4979.
9. Caspi RR. A look at autoimmunity and inflammation in the eye. *J Clin Invest*. 2010;120:3073-3083.
10. Bajwa A, Osmanzada D, Osmanzada S, et al. Epidemiology of uveitis in the mid-Atlantic United States. *Clin Ophthalmol*. 2015;9:889-901.
11. Tsirouki T, Dastiridou A, Symeonidis C, et al. A focus on the epidemiology of uveitis. *Ocul Immunol Inflamm*. 2018;26:2-16.
12. Dick AD, Tundia N, Sorg R, et al. Risk of ocular complications in patients with noninfectious intermediate uveitis, posterior uveitis, or panuveitis. *Ophthalmology*. 2016;123:655-662.
13. Chen L, Holland GN, Yu F, et al. Associations of seroreactivity against crystallin proteins with disease activity and cataract in patients with uveitis. *Invest Ophthalmol Vis Sci*. 2008;49:4476-4481.
14. Richardson RB, Ainsbury EA, Prescott CR, Lovicu FJ. Etiology of posterior subcapsular cataracts based on a review of risk factors including aging, diabetes, and ionizing radiation. *Int J Radiat Biol*. 2020;96:1339-1361.
15. Ozates S, Berker N, Cakar Ozdal P, Ozdamar Erol Y. Phacoemulsification in patients with uveitis: long-term outcomes. *BMC Ophthalmol*. 2020;20:109.
16. Llop SM, Papaliodis GN. Cataract surgery complications in uveitis patients: a review article. *Semin Ophthalmol*. 2018;33:64-69.
17. Pålsson S, Andersson Grönlund M, Skiljic D, Zetterberg M. Phacoemulsification with primary implantation of an intraocular lens in patients with uveitis. *Clin Ophthalmol*. 2017;11:1549-1555.
18. Wormstone IM, Wormstone YM, Smith AJO, Eldred JA. Posterior capsule opacification: what's in the bag? *Prog Retin Eye Res*. 2020;82:100905.
19. Tamm ER. The trabecular meshwork outflow pathways: structural and functional aspects. *Exp Eye Res*. 2009;88:648-655.
20. Ji Y, Rong X, Ye H, Zhang K, Lu Y. Proteomic analysis of aqueous humor proteins associated with cataract development. *Clin Biochem*. 2015;48:1304-1309.
21. Carreon T, van der Merwe E, Fellman RL, Johnstone M, Bhattacharya SK. Aqueous outflow - a continuum from trabecular meshwork to episcleral veins. *Prog Retin Eye Res*. 2017;57:108-133.
22. Bos KJ, Holmes DF, Kadler KE, McLeod D, Morris NP, Bishop PN. Axial structure of the heterotypic collagen fibrils of vitreous humour and cartilage. *J Mol Biol*. 2001;306:1011-1022.
23. Bishop PN. Structural macromolecules and supramolecular organisation of the vitreous gel. *Prog Retin Eye Res*. 2000;19:323-344.
24. DeDreu J, Bowen CJ, Logan CM, et al. An immune response to the avascular lens following wounding of the cornea involves ciliary zonule fibrils. *FASEB J*. 2020;34:9316-9336.

25. Logan CM, Bowen CJ, Menko AS. Induction of immune surveillance of the dysmorphogenic lens. *Sci Rep*. 2017;7:16235.
26. Prieto-Del-Cura M, González-Guijarro JJ. Risk factors for ocular complications in adult patients with uveitis. *Eur J Ophthalmol*. 2020;30:1381-1389.
27. Sun Y, Ji Y. A literature review on Fuchs uveitis syndrome: an update. *Surv Ophthalmol*. 2020;65:133-143.
28. Blum-Hareuveni T, Seguin-Greenstein S, Kramer M, et al. Risk factors for the development of cataract in children with uveitis. *Am J Ophthalmol*. 2017;177:139-143.
29. Caspi RR. Experimental autoimmune uveoretinitis in the rat and mouse. *Curr Protoc Immunol Chapter*. 2003;15:Unit 15.16.
30. Mattapallil MJ, Silver PB, Cortes LM, et al. Characterization of a new epitope of IRBP that induces moderate to severe uveoretinitis in mice with H-2b haplotype. *Invest Ophthalmol Vis Sci*. 2015;56:5439-5449.
31. Klaassen I, Van Noorden CJ, Schlingemann RO. Molecular basis of the inner blood-retinal barrier and its breakdown in diabetic macular edema and other pathological conditions. *Prog Retin Eye Res*. 2013;34:19-48.
32. Runkle EA, Antonetti DA. The blood-retinal barrier: structure and functional significance. *Methods Mol Biol*. 2011;686:133-148.
33. van der Wijk AE, Wisniewska-Kruk J, Vogels IMC, et al. Expression patterns of endothelial permeability pathways in the development of the blood-retinal barrier in mice. *FASEB J*. 2019;33:5320-5333.
34. Crabtree E, Song L, Llanga T, et al. AAV-mediated expression of HLA-G1/5 reduces severity of experimental autoimmune uveitis. *Sci Rep*. 2019;9:19864.
35. Chen J, Qian H, Horai R, Chan CC, Falick Y, Caspi RR. Comparative analysis of induced vs. spontaneous models of autoimmune uveitis targeting the interphotoreceptor retinoid binding protein. *PLoS ONE*. 2013;8:e72161.
36. Agarwal RK, Caspi RR. Rodent models of experimental autoimmune uveitis. *Methods Mol Med*. 2004;102:395-419.
37. Chong WP, Mattapallil MJ, Raychaudhuri K, et al. The cytokine IL-17A limits Th17 pathogenicity via a negative feedback loop driven by autocrine induction of IL-24. *Immunity*. 2020;53:384-397.e385.
38. Demir I, Westermann R. Vector-to-closest-point octree for surface ray-casting. In: Bommes D, Ritschel T, Schultz T, eds. *Vision, Modeling, and Visualization*. The Eurographics Association; 2015:65-72.
39. DeDreu J, Walker JL, Menko AS. Dynamics of the lens basement membrane capsule and its interaction with connective tissue-like extracapsular matrix proteins. *Matrix Biol*. 2021;96:18-46.
40. Napier RJ, Lee EJ, Davey MP, et al. T cell-intrinsic role for Nod2 in protection against Th17-mediated uveitis. *Nat Commun*. 2020;11:5406.
41. Saunders AE, Johnson P. Modulation of immune cell signalling by the leukocyte common tyrosine phosphatase, CD45. *Cell Signal*. 2010;22:339-348.
42. Evans R, Patzak I, Svensson L, et al. Integrins in immunity. *J Cell Sci*. 2009;122:215-225.
43. Mecham RP, Gibson MA. The microfibril-associated glycoproteins (MAGPs) and the microfibrillar niche. *Matrix Biol*. 2015;47:13-33.
44. Pepple KL, Wilson L, Van Gelder RN. Comparison of aqueous and vitreous lymphocyte populations from two rat models of experimental uveitis. *Invest Ophthalmol Vis Sci*. 2018;59:2504-2511.
45. Ghosh S, Hernando N, Martín-Alonso JM, Martin-Vasallo P, Coca-Prados M. Expression of multiple Na^+, K^+-ATPase genes reveals a gradient of isoforms along the nonpigmented ciliary epithelium: functional implications in aqueous humor secretion. *J Cell Physiol*. 1991;149:184-194.
46. Jones W, Rodriguez J, Bassnett S. Targeted deletion of fibrillin-1 in the mouse eye results in ectopia lentis and other ocular phenotypes associated with Marfan syndrome. *Dis Model Mech*. 2019;12:dmm037283.
47. Chan CC, Caspi RR, Ni M, et al. Pathology of experimental autoimmune uveoretinitis in mice. *J Autoimmun*. 1990;3:247-255.
48. Lee EJ, Brown BR, Vance EE, et al. Mincle activation and the Syk/Card9 signaling axis are central to the development of autoimmune disease of the eye. *J Immunol*. 2016;196:3148-3158.
49. Chen M, Zhao J, Ali IHA, et al. Cytokine signaling protein 3 deficiency in myeloid cells promotes retinal degeneration and angiogenesis through arginase-1 up-regulation in experimental autoimmune uveoretinitis. *Am J Pathol*. 2018;188:1007-1020.
50. Tu Z, Li Y, Smith D, et al. Myeloid suppressor cells induced by retinal pigment epithelial cells inhibit autoreactive T-cell responses that lead to experimental autoimmune uveitis. *Invest Ophthalmol Vis Sci*. 2012;53:959-966.
51. Diacovo TG, Roth SJ, Buccola JM, Bainton DF, Springer TA. Neutrophil rolling, arrest, and transmigration across activated, surface-adherent platelets via sequential action of P-selectin and the beta 2-integrin CD11b/CD18. *Blood*. 1996;88:146-157.
52. Bednarczyk M, Stege H, Grabbe S, Bros M. β2 integrins-multifunctional leukocyte receptors in health and disease. *Int J Mol Sci*. 2020;21(4):1402.
53. Jakoš T, Pišlar A, Jewett A, Kos J. Cysteine cathepsins in tumor-associated immune cells. *Front Immunol*. 2019;10:2037.
54. Wight TN, Frevert CW, Debley JS, Reeves SR, Parks WC, Ziegler SF. Interplay of extracellular matrix and leukocytes in lung inflammation. *Cell Immunol*. 2017;312:1-14.
55. Vafadari B, Salamian A, Kaczmarek L. MMP-9 in translation: from molecule to brain physiology, pathology, and therapy. *J Neurochem*. 2016;139(suppl 2):91-114.
56. Heissig B, Nishida C, Tashiro Y, et al. Role of neutrophil-derived matrix metalloproteinase-9 in tissue regeneration. *Histol Histopathol*. 2010;25:765-770.
57. Gery I, Caspi RR. Tolerance induction in relation to the eye. *Front Immunol*. 2018;9:2304.
58. Dustin ML. Integrins and their role in immune cell adhesion. *Cell*. 2019;177:499-501.
59. Zhang Y, Wang H. Integrin signalling and function in immune cells. *Immunology*. 2012;135:268-275.
60. Smigiel KS, Parks WC. Matrix metalloproteinases and leukocyte activation. *Prog Mol Biol Transl Sci*. 2017;147:167-195.
61. Ohlmann AV, Ohlmann A, Welge-Lüssen U, May CA. Localization of collagen XVIII and endostatin in the human eye. *Curr Eye Res*. 2005;30:27-34.
62. Harkness LM, Weckmann M, Kopp M, Becker T, Ashton AW, Burgess JK. Tumstatin regulates the angiogenic and inflammatory

potential of airway smooth muscle extracellular matrix. *J Cell Mol Med*. 2017;21:3288-3297.
63. Mongiat M, Sweeney SM, San Antonio JD, Fu J, Iozzo RV. Endorepellin, a novel inhibitor of angiogenesis derived from the C terminus of perlecan. *J Biol Chem*. 2003;278:4238-4249.
64. Neill T, Kapoor A, Xie C, Buraschi S, Iozzo RV. A functional outside-in signaling network of proteoglycans and matrix molecules regulating autophagy. *Matrix Biol*. 2021;100-101:118-149.
65. Walia A, Yang JF, Huang YH, Rosenblatt MI, Chang JH, Azar DT. Endostatin's emerging roles in angiogenesis, lymphangiogenesis, disease, and clinical applications. *Biochim Biophys Acta*. 2015;1850:2422-2438.
66. Guo T, Zou L, Ni J, et al. Regulatory T cells: an emerging player in radiation-induced lung injury. *Front Immunol*. 2020;11:1769.
67. Stepp MA, Menko AS. Immune responses to injury and their links to eye disease. *Transl Res*. 2021;236:52-71.

SUPPORTING INFORMATION

Additional Supporting Information may be found in the online version of the article at the publisher's website.

How to cite this article: DeDreu J, Pal-Ghosh S, Mattapallil MJ, Caspi RR, Stepp MA, Menko AS. Uveitis-mediated immune cell invasion through the extracellular matrix of the lens capsule. *FASEB J*. 2022;36:e21995. doi:10.1096/fj.202101098R